26.8 A 236nW -56.5dBm-Sensitivity Bluetooth Low-Energy Wakeup Receiver with Energy Harvesting in 65nm CMOS

Nathan E. Roberts[1], Kyle Craig[1], Aatmesh Shrivastava[1], Stuart N. Wooters[1], Yousef Shakhsheer[1], Benton H. Calhoun[1], David D. Wentzloff[2]

[1]PsiKick, Charlottesville, VA, [2]PsiKick, Ann Arbor, MI

Batteryless operation and ultra-low-power (ULP) wireless communication will be two key enabling technologies as the IC industry races to keep pace with the IoE projections of 1T-connected sensors by 2025. Bluetooth Low-Energy (BLE) is used in many consumer IoE devices now because it offers the lowest average power for a radio that can communicate directly to a mobile device [1]. The BLE standard requires that the IoE device continuously advertises, which initiates the connection to a mobile device. Sub-1s advertisement intervals are common to minimize latency. However, this continuous advertising results in a typical minimum average power of 10's of µW at low duty-cycles. This leads to the quoted 1-year lifetimes of event-driven IoE devices (e.g. tracking tags, ibeacons) that operate from coin-cell batteries. This minimum power is too high for robust, batteryless operation in a small form-factor.

Wakeup radios (WRX) are a viable solution that invert the networking topology by having the mobile device initiate the connection (Fig. 26.8.1), reducing the minimum average power on the IoE device. However, recently reported WRXs require a custom wakeup signal that cannot be produced by a standard-compliant radio [2,3]. This paper introduces the concept of back-channel communication from a BLE-compliant transmitter to a ULP WRX. A 236nW WRX is presented that wakes up from standard-compliant BLE advertisements on a mobile device (Fig. 26.8.1). The WRX includes a broadband, non-coherent RF front-end with low- and high-sensitivity paths, automatic interference rejection, and a 32kHz crystal oscillator. An energy-harvesting power-management unit (EH-PMU) enables batteryless operation and includes a band-gap reference and brownout detection. The integrated baseband processor operates in sub-V_t and includes a modem supporting three wakeup modes.

Back-channel modulation enables a standard-compliant BLE radio to communicate to a ULP, energy-detection receiver. This is achieved by controlling the BLE radio within the constraints of the standard to produce signals that a ULP, energy-detection receiver can demodulate to recover the back-channel information. Figure 26.8.2 summarizes the BLE advertising protocol according to the standard. Individual advertising packets range from 128 to 376us, depending on payload length. An advertising event comprises three packets in succession, <10ms apart, one on each of the three advertising channels. When in advertising mode, advertising events are broadcast at an interval programmable from 20ms to 10.24s. A 0-to-10ms pseudo-random delay time is added to minimize collisions. BLE advertising is supported on most mobile devices, but with restrictions on what can be controlled through the operating system. However, the advertising interval and the time duration of advertising are easily controlled through APIs. Back-channel information can therefore be encoded onto the advertising interval and duration (Fig. 26.8.2) on a mobile device, requiring only a software change (new app) to generate a wakeup message. An energy-detection WRX then detects the presence of all packets in the 2.4GHz band. This feeds into a baseband processor that correlates the energy levels with a time-based template that matches the expected sequence of BLE advertising packets to determine the presence of a back-channel wakeup message.

The receiver front-end (Fig. 26.8.3) consists of an off-chip 2-element matching network with a passive RF rectifier [3]. Following the rectifier the signal path splits into three different blocks: RF harvesting and two receive paths. In the default startup condition, before the PMU rails are established, a switch between the rectifier and VCAP is closed allowing the storage capacitor to be charged by an RF signal if desired. Once the baseband processor is powered up and reset, this switch is automatically opened so the chip can operate in RF reception mode.

The low-sensitivity receive path contains a dynamic latched-based comparator (Fig. 26.8.3) directly following the rectifier. Programmable weighting can be applied to either the inputs or the cross-coupled inverters, which changes the threshold of the comparator. Adjusting it higher requires a larger signal to trip the comparator, which reduces sensitivity, but also prevents high-power interferers from saturating the receiver. The high-sensitivity path adds fixed- and variable-gain amplifiers followed by a similar latch-based comparator. Gain is tunable from 20 to 45dB. Finally, the 2.4GHz band is shared with many other transmitters. The threshold of the comparator is automatically adjusted based on the interference levels. If a consecutive number of 1s or 0s is detected, then the automatic threshold controller will raise or lower the comparator threshold, respectively. The receiver has its highest sensitivity when the channel is quiet, and trades off sensitivity for interference rejection when the channel is noisy.

The sub-V_t digital baseband processor includes the back-channel modem, which supports multiple wake-up modes, two 32-bit timers, a reset handler, and an interrupt handler. The interrupt handler manages the interrupts received from the modem, timer, or reset handler. The wake-up modem receives back-channel messages from a BLE-compliant device and asserts an interrupt when a wake-up message is received. The 1-bit comparator output is fed to the modem, which uses multiple correlators to detect the presence of BLE advertisements and measure the packet rate, length, and advertisement duration. This is decoded into a string of symbols according to the back-channel protocol, which are checked against a programmable address and an interrupt asserted when there is a match. Finally, memory-mapped registers, configurable over SPI, configure the baseband processor and report the status of the chip.

The EH-PMU (Fig. 26.8.4) consists of an energy-harvester circuit to harvest energy down to DC voltage levels of 30mV. It also includes a single-inductor multiple-output (SIMO) PMU that regulates three output voltages. The EH-PMU is specifically designed to acquire sub-microwatt to several milliwatts of power generated from DC energy harvesting sources such as photovoltaic cells (PV) or thermoelectric generators (TEG), and support ULP to high loads at the output. The energy harvester supports a cold-start mode during start-up, RF energy-harvesting mode, and normal boost operation. The cold-start mode enables start-up of the EH-PMU and charges VCAP to 850mV, which initiates normal operation [4] where the boost converter can efficiently charge from VIN greater than 30mV. The energy harvester can also charge from RF signals in the ISM band in its RF harvesting mode with a sensitivity of -7dBm. The boost converter uses a programmable maximum-power-point-tracking (MPPT) sampling network to maximize the input power from the harvester. The maximum power point for different harvesters is programmed with sampling resistors R_{SAMPH} and R_{SAMPL}. The EH-PMU also generates three output rails to provide a 0.5V rail for digital and RF, a 1.0V rail for high-performance digital, and a 2.5V rail for I/O communication.

The chip was fabricated in a 65nm LP CMOS process. The EH-PMU supports 5V storage and boost operation using a 2.5V gate-oxide, drain-extended transistor. The bias voltages and LDO to support high-voltage operation are controlled using a ULP bandgap reference [5]. The quiescent current of the EH-PMU is 350nA at 0.85V VCAP. Figure 26.8.4 shows the measured waveform of the EH-PMU starting up from 350mV VIN to charge VCAP to 5V and generate three regulated output voltages. Figure 26.8.5 shows the efficiency measurement of the boost converter across VIN and VCAP voltages, with a peak efficiency of 96%. The peak efficiency of the SIMO regulator is 83%. Figure 26.8.5 shows the raw error-rate taken at the output of the comparator in the low-sensitivity path. The chip-rate of the receiver is 8.192kb/s. Power and sensitivity of the receiver in low- and high-sensitivity modes are 104nW and 236nW, and -39dBm and -56.5dBm, respectively, which includes the RF front-end, baseband processor, and 32kHz clock. These sensitivities were measured when waking up from 31-bit codes, and include all processing gain in the modem. Figure 26.8.5 shows the comparator output due to a back-channel code sent from an iPhone, along with the external interrupt signal demonstrating a wakeup event. Figure 26.8.6 is a comparison table.

Acknowledgements: The authors thank Osama Khan for contributions to the circuit design.

References:

[1] J. Prummel et al., "A 10mW Bluetooth Low-Energy Transceiver with On-Chip Matching," *ISSCC Dig. Tech. Papers*, pp. 238-239, Feb. 2015.

[2] C. Salazar et al., "A -97dBm-Sensitivity Interferer-Resilient 2.4GHz Wake-Up Receiver Using Dual-IF Multi-N-Path Architecture in 65nm CMOS," *ISSCC Dig. Tech. Papers*, pp. 242-243, Feb. 2015.

[3] S. Oh, N. Roberts and D.D. Wentzloff, "A 116nW multi-band wake-up receiver with 31-bit correlator and interference rejection," *IEEE Custom Integrated Circuits Conf.*, pp. 1-4, Sept. 2013.

[4] A. Shrivastava et al., "A 10 mV-input Boost Converter with Inductor Peak Current Control and Zero Detection for Thermoelectric and Solar Energy Harvesting with 220 mV Cold-Start and -14.5dBm, 915 MHz RF Kick-Start," *IEEE J. Solid-State Circuits*, vol. 50, no. 8, pp. 1820-1832, Aug. 2015.

[5] A. Shrivastava et al., "A 32nW bandgap reference voltage operational from 0.5 V supply for ultra-low power systems," *ISSCC Dig. Tech. Papers*, pp. 1-3, Feb. 2015.

 978-1-4673-9467-3/16/$31.00

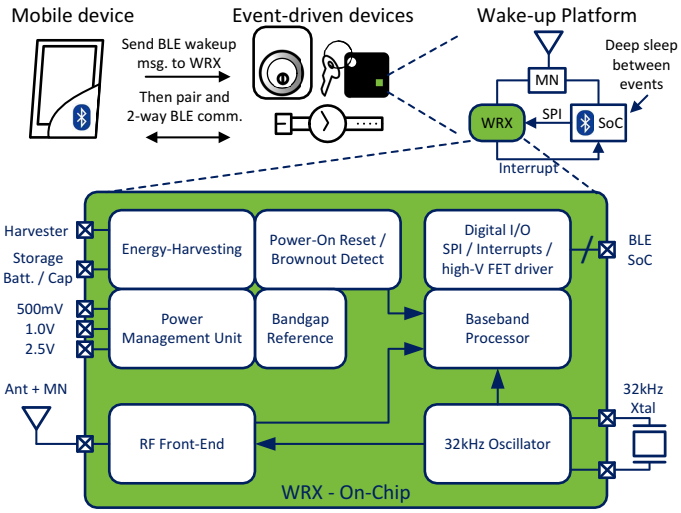

Figure 26.8.1: Application example of an event-driven wakeup using back-channel over BLE, and block diagram of the wakeup radio.

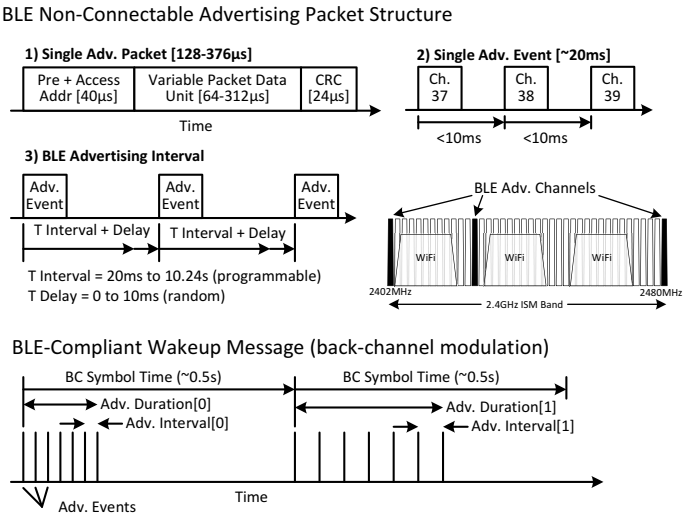

Figure 26.8.2: Wakeup message format encoding back-channel information generated by a BLE-compliant radio and detectable by a ULP WRX.

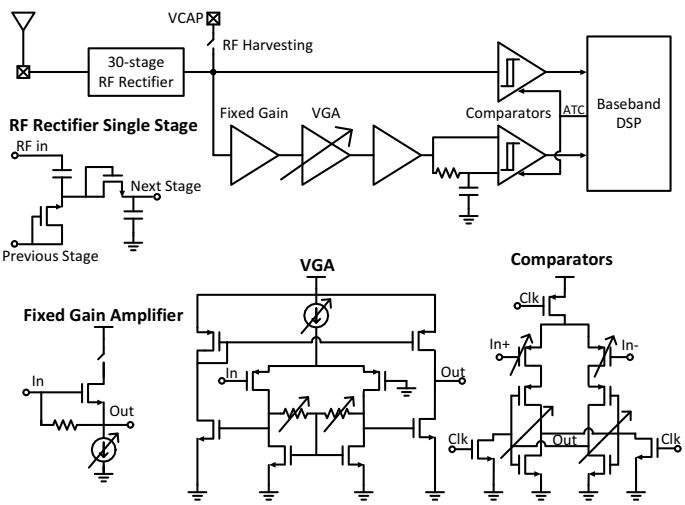

Figure 26.8.3: RF front-end circuits showing low- and high-sensitivity paths.

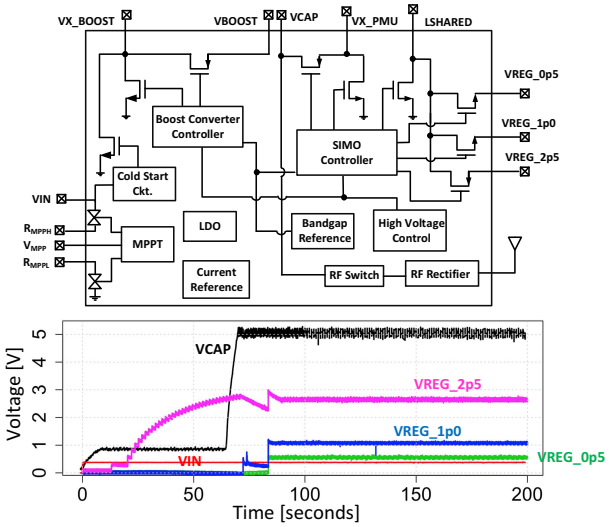

Figure 26.8.4: Energy-harvesting power-management unit and its measured startup waveform.

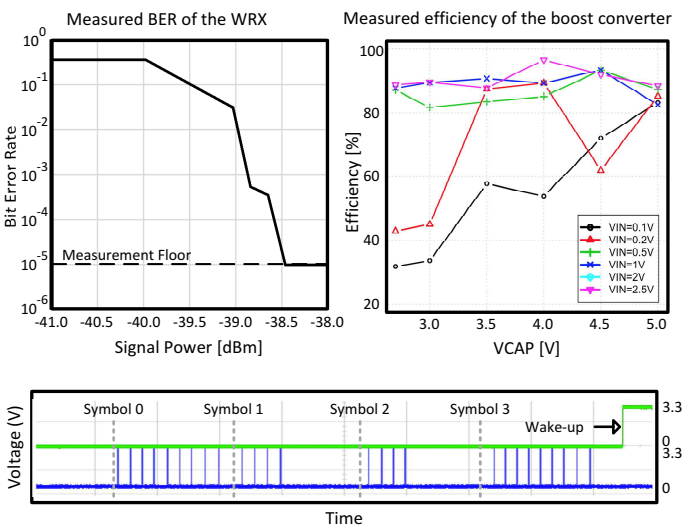

Figure 26.8.5: Chip error-rate of the comparator output of the low-sens RX path. Boost converter efficiency. Measured back-channel message from iPhone.

	This Work	[Klinefelter ISSCC'15]	[Lee JSSC-Jan'13]	[Abe VLSI'14]	[4]
Active Power	580nW	6.45µW	40µW	45.5µW	300nW
Function	WRX	IoT Node	Sensor	WRX	Harvester
Integrated PMU	✓	✓	✓	×	×
EH-Types	PV, TEG, RF	PV, TEG	PV, TEG, FC	-	PV, TEG, RF
EH-Efficiency	96%	74.9%	26.9%	-	83%
Regulator Eff.	83%		62%	-	-
Reg. Output (V)	0.5, 1.0, 2.5	0.5, 1.0, 1.2, Var	0.6, 1.2	-	-
SIMO Reg.	✓	✓	Switch Cap.	×	×
Batt. Mgmt.	✓	×	✓	×	✓
Min. Boost Volt.	30mV	30mV	307mV	-	10mV
Cold Start	300mV	300mV	-	-	220mV
RF-EH Sens.	-7 dBm	-	-	-	-14.5 dBm
Integrated Tx/Rx	Rx	Rx/Tx	×	Rx	×
Rx Sens. (low/hi)	-39/56dBm	-41dBm	-	-87dBm	-
Rx Center Freq.	0.4-2.4GHz	0.4-2.4GHz	-	924.4MHz	-
Rx Data Rate	8.192kbps	7.8125kbps	-	50kbps	-
Rx Power (low/hi)	104/236nW	112nW	-	45.5µW	-
WRX Supply	0.5V,1.0V	0.5V	-	0.7	-
WRX Protocol	BLS/CDMA	CDMA	-	GFSK	-
Technology	65nm	130nm	65nm,180nm	65nm	130nm
Die Area	2.25mm²	13.49mm²	6.05mm²	1.27mm²	0.12mm²
Max Voltage	5V	1.4V	4.2V	-	1.2V

FC=Microbial Fuel Cell, Var=Programmable Supply

Figure 26.8.6: Performance and system comparison table.

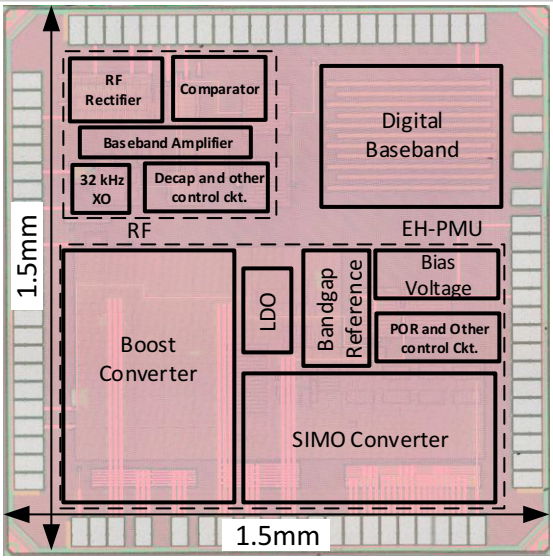

Figure 26.8.7: Die micrograph.

978-1-4673-9467-3/16/$31.00 ©2016 IEEE